

STATUS AND RECENT RESULTS OF THE BAIKAL-GVD PROJECT

*A. D. Avrorin*¹, *A. V. Avrorin*¹, *V. M. Aynutdinov*¹, *R. Bannasch*⁷,
*I. A. Belolaptikov*², *D. Yu. Bogorodsky*³, *V. B. Brudanin*²,
*N. M. Budnev*³, *I. A. Danilchenko*¹, *G. V. Domogatsky*¹,
*A. A. Doroshenko*¹, *A. N. Dyachok*³, *Zh.-A. M. Dzilhikibaev*^{1,*},
*S. V. Fialkovsky*⁵, *A. R. Gafarov*³, *O. N. Gaponenko*¹,
*K. V. Golubkov*¹, *T. I. Gress*³, *Z. Hons*², *K. G. Kebkal*⁷,
*O. G. Kebkal*⁷, *K. V. Konishchev*², *E. N. Konstantinov*³,
*A. V. Korobchenko*³, *A. P. Koshechkin*¹, *F. K. Koshel*¹,
*V. A. Kozhin*⁴, *V. F. Kulepov*⁵, *D. A. Kuleshov*¹, *V. I. Ljashuk*¹,
*M. B. Milenin*⁵, *R. A. Mirgazov*³, *E. R. Osipova*⁴, *A. I. Panfilov*¹,
*L. V. Pankov*³, *A. A. Perevalov*³, *E. N. Pliskovsky*²,
*V. A. Poleshuk*³, *M. I. Rozanov*⁶, *V. F. Rubtsov*³, *E. V. Rjabov*³,
*B. A. Shaybonov*², *A. A. Sheifler*¹, *A. V. Skurikhin*⁴, *A. A. Smagina*²,
*O. V. Suvorova*¹, *B. A. Tarashchansky*³, *S. A. Yakovlev*⁷,
*A. V. Zagorodnikov*³, *V. A. Zhukov*¹, *V. L. Zurbanov*³

¹ Institute for Nuclear Research, Moscow

² Joint Institute for Nuclear Research, Dubna

³ Irkutsk State University, Irkutsk, Russia

⁴ Skobeltsyn Institute of Nuclear Physics, Moscow State University, Moscow

⁵ Nizhni Novgorod State Technical University, Nizhni Novgorod, Russia

⁶ St. Petersburg State Marine University, St. Petersburg, Russia

⁷ EvoLogics GmbH, Berlin

The prototyping phase of the BAIKAL-GVD project was started in April 2011 with the deployment of first autonomous engineering array which comprises all basic elements and systems of the Gigaton Volume Detector (GVD) in Lake Baikal. The prototyping phase will be concluded with deployment of the GVD demonstration cluster "DUBNA" in 2015, which will comprise 192 light sensors arranged at 8 strings. The first stage of the GVD demonstration cluster which consists of three strings was deployed in April

*Corresponding author, djilkib@pcbai10.inr.ruhep.ru

2013 and successfully operated up to February 2014. We review the prototyping phase of the BAIKAL-GVD project and describe the configuration and design of the 2013 engineering array.

PACS: 29.40.Ka; 98.70.Sa; 14.60.Lm

INTRODUCTION

The BAIKAL-GVD project is a logical extension of the research and development work performed over the last several years by the BAIKAL Collaboration. The optical properties of the lake deep water have been established [1], and the detection of high-energy neutrinos has been demonstrated with the detector NT200 [2, 3]. This achievement represents a proof of concept for commissioning the new instrument, Gigaton Volume Detector (BAIKAL-GVD), with superior detector performance and an effective telescope size at or above the kilometer-scale. The next-generation neutrino telescope BAIKAL-GVD in Lake Baikal will be a research infrastructure aimed primarily at studying astrophysical neutrino fluxes and particularly at mapping the high-energy neutrino sky in the Southern Hemisphere including the region of the galactic center. The detector will utilize Lake Baikal water instrumented at depth with light sensors that detect the Cherenkov radiation from secondary particles produced in interactions of high-energy neutrinos inside or near the instrumented water volume. The site chosen for the experiment is in the southern basin of Lake Baikal. Here combination of hydrological, hydrophysical, and landscape factors is optimal for deployment and operation of the neutrino telescope. Lake depth is about 1360 m here at distances beginning from about three kilometers from the shore. The flat lake bed throughout several tens of kilometers from the shore allows practically unlimited instrumented water volume for deep underwater Cherenkov detector. A strong up to 1 m thick ice cover from February to the middle of April allows telescope deployment, as well as maintenance and research works directly from the ice surface, using it like a solid and fixed assembling platform. The light propagation in the Baikal water is characterized by an absorption length of about 20–25 m and a scattering length of 30–50 m. The water luminescence is moderate at the detector site. The first-generation Baikal Neutrino Telescope NT200 has been operating in Lake Baikal since April 1998 [4–6]. The upgraded Baikal telescope NT200+ was commissioned in April 2005, and consists of central part (the former, densely instrumented NT200 telescope) and three additional external strings. The deployment of the NT200+ was a first step towards a km³-scale neutrino telescope in Lake Baikal. The first prototype of the GVD electronics was installed in Lake Baikal in April 2008 [7]. It was reduced-size section with 6 optical modules (OMs). This detection unit provided the possibility to study basic elements of the future detector: new optical modules and Flash Analog-to-Digital Converter

(FADC) based measuring system. During the next two years different versions of prototype string were tested in Lake Baikal as a part of the NT200+ detector. The 2009 prototype string consists of 12 optical modules with six photomultiplier tubes (PMTs) R8055 and six XP1807 [8,9]. In April 2010, the string with 8 PMTs R7081HQE and 4 PMTs R8055 was deployed in Lake Baikal. The operation of these prototype strings in 2009 and 2010 allows first assessment of the DAQ performance [10, 11, 15].

1. GVD DESIGN

The BAIKAL-GVD is a 3-dimensional lattice of photomultiplier tubes each enclosed in a transparent pressure sphere to comprise an optical module. The OMs are arranged on vertical load-carrying cables to form strings. The configuration of telescope consists of clusters of strings — functionally independent subarrays, which are connected to shore by individual electro-optical cables (see Fig. 1). Each cluster comprises eight strings of optical modules — seven peripheral strings are uniformly arranged at a 60 m distance around a central one. Optical modules are spaced by 15 m along each string and are faced downward. OMs on each string are combined in sections — detection units of telescope. The distances between the central strings of neighboring clusters are 300 m.

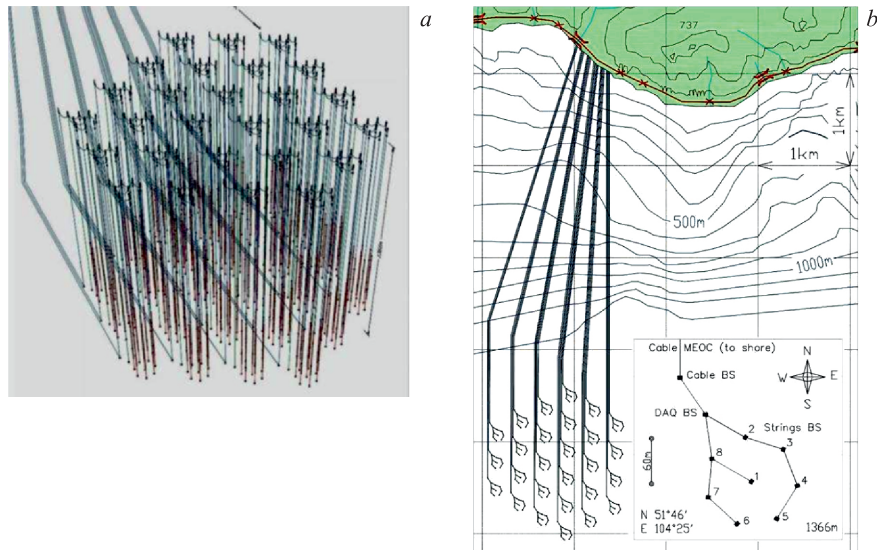


Fig. 1. *a)* Artistic view of the GVD telescope. *b)* Layout of the GVD. In inner box layout of the GVD cluster is shown

Muon effective areas for two optimized GVD configurations are shown in Fig. 2, *a*. The curves labeled by GVD*4 and GVD relate to configurations with 10368 OMs and 2304 OMs, respectively. Muon effective area for GVD*4 (6/3 event selection requirement — at least 6 hit channels on at least 3 strings) rises from 0.3 km^2 at 1 TeV to about 1.8 km^2 asymptotically. The fraction of events induced by muons ($E_\mu > 1 \text{ TeV}$) with mismatch angles between generated and reconstructed muon directions less than a given value ψ is shown in Fig. 2, *b*. Muon arrival direction resolution (median mismatch angle) is about 0.25 deg.

Shower effective volumes for two GVD configurations are shown in Fig. 3, *a*. Shower effective volumes (11/3 condition — at least 11 hit channels on at least 3 strings) for GVD*4 are about $0.4\text{--}2.4 \text{ km}^3$ above 10 TeV. The accuracy of

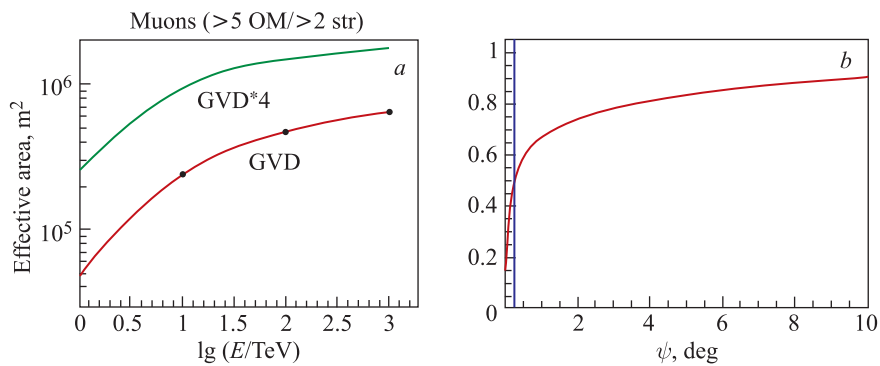


Fig. 2. *a*) Muon effective area. The curves labeled by GVD*4 and GVD relate to configurations with 10368 OMs and 2304 OMs, respectively. *b*) The fraction of muon events ($E_\mu > 1 \text{ TeV}$) with mismatch angle ψ less than a given value

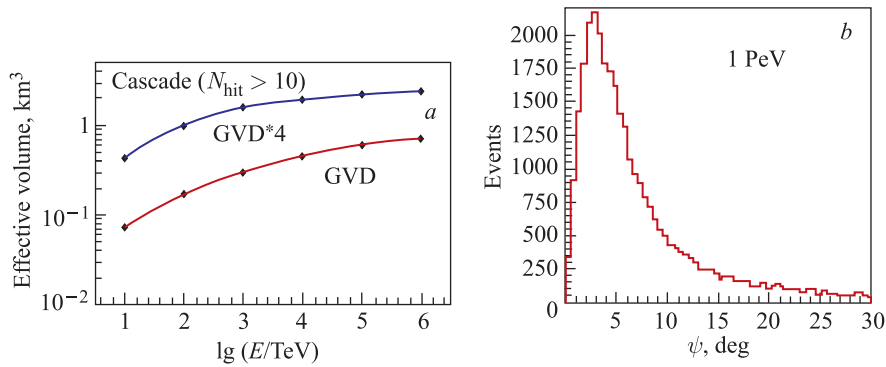


Fig. 3. *a*) Effective volume of cascades detection. The curves labeled by GVD*4 and GVD relate to configurations with 10368 OMs and 2304 OMs, respectively. *b*) Distribution of the mismatch angle ψ between generated and reconstructed 1 PeV shower directions

shower energy reconstruction is about 20–35% depending on shower energy. Shower angular resolution is about 3.5–6.5 deg (median value). Distribution of the mismatch angle between generated and reconstructed directions of 1 PeV showers is shown in Fig. 3, *b*.

2. DEMONSTRATION CLUSTER “DUBNA”

The prototyping and early construction phase of the BAIKAL-GVD project aims at in situ comprehensive tests of all elements and systems of the future telescope as the parts of engineering arrays operating in Lake Baikal. Prototyping phase will be concluded with deployment in 2015 of the first demonstration cluster of the GVD in Lake Baikal. The demonstration cluster will comprise a total of 192 optical modules arranged on eight 345 m long strings (7 side strings located at 60 m distances from a central one). Each string comprises 24 OMs spaced by 15 m at depths of 900 to 1250 m below the surface. OMs on each string are combined in two sections. Also the demonstration cluster will comprise an acoustic positioning system and an instrumentation string with equipment for array calibration and monitoring of environment parameters. The demonstration cluster will be connected to shore by the electro-optical cable.

2.1. Optical Module. Each optical module consists of a pressure-resistant glass sphere with 42 cm diameter which holds OM electronics and PMT surrounded by a high permittivity alloy cage for shielding it against Earth’s magnetic field (see Fig. 4, *a*). A large photomultiplier tube Hamamatsu R7081HQE is selected as a light sensor of OM. This PMT has a hemispherical photocathode with 10-inch diameter and high quantum efficiency up to 35% (see Fig. 4, *b*). Besides the PMT, an OM comprises a high-voltage power supply unit (HV), a fast two-channel preamplifier, and a controller. The HV unit provides the volt-

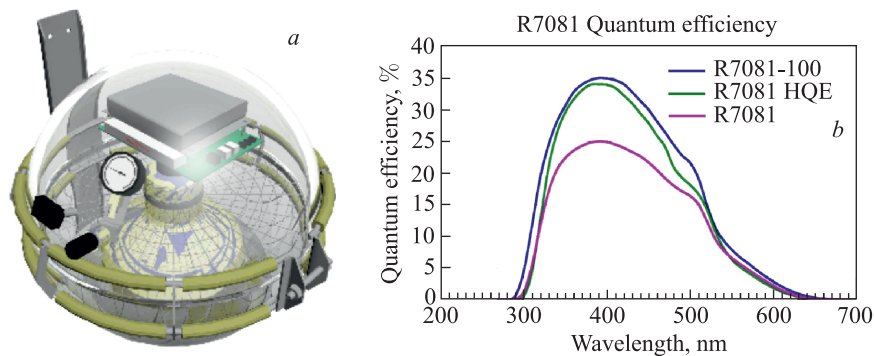


Fig. 4. *a*) Optical module. *b*) Quantum efficiency of PMT. Two upper curves relate to PMTs with high quantum efficiency

age for the phototube divider up to 2 kV. The tube gain has been adjusted to about 10^7 . An additional signal amplification by a factor of 10 is provided by the first channel of the preamplifier. This gain value results in a spectrometric channel linearity range up to about 100 photoelectrons. The second preamplifier output with factor 20 is intended for PMT noise monitoring. For temporal and amplitude calibration of the measuring channel, two LEDs are installed in the optical module. The dominant wavelength of the LED is 445 nm, the LED pulse has a width of about 5 ns (FWHM). The possibility of independent regulation of the LED light intensity and low crosstalk between LED channels ($< 1\%$) allows direct measurement of the linearity range of the spectrometric channel. The OM controller is intended for HV control and monitoring, for PMT noise measurements, and for time and amplitude calibration. The OM controller is designed on the basis of the microcontroller SiLabs C8051F121. Slow control data to and from the OMs are transferred via an underwater RS-485 bus.

2.2. Data Acquisition. The optical modules are grouped into sections — the detection units of array [7–11]. Each section includes 12 OMs and the central module (CeM). PMTs signals from all OMs are transmitted through 90 m long coaxial cables to the central module of the section, where they are digitized by custom-made ADC boards with 200 MHz sampling rate. The waveform information from all measuring channels of the section is transferred to the Master board located in the CeM. The Master board provides data readout from ADC, connection via local Ethernet to the cluster DAQ-center, control of the section operation and the section trigger logic [7–11]. Request of the section trigger is transferred from the Master board to the cluster DAQ-center, where a global trigger for all sections is formed. The global trigger initiates data transmission from all sections to shore.

Data collected in section central modules are transmitted to shore through three different parts of the underwater communication network based on Ethernet. The section communication channels connect each CeM with the corresponding string communication module (CoM). Given the lengths of these communication channels of more than 100 m, the shDSL modems are used as the Ethernet extensions for data transmission from CeM to CoM. In CoM the section communication channels are joined into a single one, which connects each section with the cluster DAQ-center. Data transmission between each CoM and the cluster DAQ-center is also based on shDSL technology.

The data transmission between the cluster DAQ-center and shore station is provided through 6 km long optical fibre lines. Maximal speed of data transmission to shore is limited by band width of a connection channel between a string CoM and the cluster DAQ-center and is about 8 Mbit/s. To provide the required data rate (not less than 100 Hz), on-line data processing in each section is performed. As a result, a raw data sample is reduced more than 50 times, since the data are refined by the Master electronic cards located in CeMs.

2.3. Slow Control. The basic functions of control and monitoring of the array recording system are realized by OMs controllers and ADC and Master boards. It means a setup of array operation mode, setting the thresholds and the data accumulating time ranges of measuring channels, PMT's gains, control and monitoring of equipment parameters and background conditions during array operation.

The cluster power supply system is realized in two levels. The first level includes the 12-channel commutator which is used for string power supply and is placed in the cluster DAQ-center. The second level is formed by the commutators of strings which are located inside the string communication modules. They provide independent switch-on/off of power supply of the string sections. This scheme of power supply provides a reliable operation of the array in a whole even if some elements of recording system like section or string would be broken. Control of OM voltage (12 VDC) in each section is processed by 12-channel relay board which is managed by Master board through RS485 bus.

2.4. The Potential Power. Recently, the IceCube Collaboration reported on results of an all-sky search for high-energy neutrino events interacting within the IceCube neutrino detector conducted between May 2010 and May 2012 [13]. The search follows up on the previous detection of two PeV neutrino events [14], with improved sensitivity and extended energy coverage down to about 30 TeV. Twenty-six additional events were observed, substantially more than expected from atmospheric backgrounds. Combined, both searches reject a purely atmospheric origin for the 28 events at the 4.3σ level. These 28 events, which include the highest energy neutrinos ever observed, have flavors, directions, and energies inconsistent with those expected from the atmospheric muon and neutrino backgrounds. These properties are, however, consistent with generic predictions for an additional component of extraterrestrial origin with (1 : 1 : 1) flavor ratio.

In this search, events were selected by the requirement that they display a vertex (shower pattern) contained within the instrumented ice volume, effectively employing the edges of the IceCube detector as a veto for down-going muons. The data are well described in this energy range by an E^{-2} neutrino spectrum with a per-flavor normalization of $E^2 F(E) = (1.2 \pm 0.4) \cdot 10^{-8} \text{ GeV} \cdot \text{cm}^{-2} \cdot \text{s}^{-1} \cdot \text{sr}^{-1}$.

The Baikal Collaboration has a long-term experience of studies of muons and neutrinos by detection and reconstruction of secondary high-energy cascades. The limits on all flavor astrophysical diffuse neutrino flux were derived from data of NT200 neutrino telescope [2, 3]. Demonstration cluster of the GVD is an array which has a potential for study of the flux of astrophysical neutrinos at a level obtained by IceCube. Neutrino effective areas for each flavor assuming an equal flux of neutrinos and antineutrinos and averaged over all arrival angles are shown in Fig. 5, *a*. These areas are about a factor of 10 less than relative areas of IceCube. The accuracy of a shower direction reconstruction is about 4 deg (median value), which is substantially better than 10 deg accuracy for the

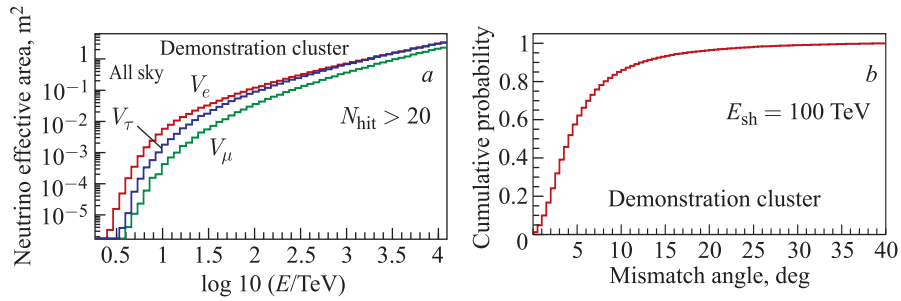


Fig. 5. *a*) Neutrino effective areas averaged over all arrival angles. *b*) The fraction of shower events with mismatch angle ψ less than a given value

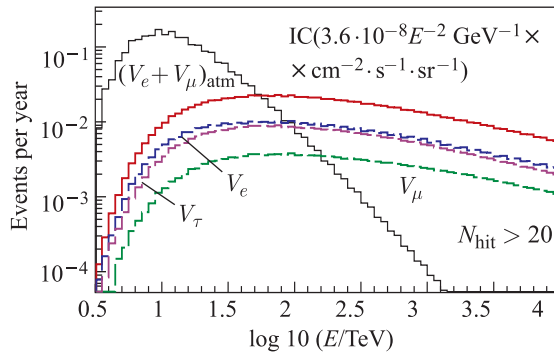


Fig. 6. Expected distributions of events from astrophysical fluxes obtained by IceCube per year. Also shown is a distribution of background events from atmospheric neutrinos

IceCube. The fraction of shower events ($E_{\text{sh}} = 100 \text{ TeV}$) with mismatch angles between generated and reconstructed shower directions less than a given value ψ is shown in Fig. 5, *b*. Energy distributions of expected shower events per year from IceCube astrophysical neutrino fluxes for different flavors and all-flavor flux, as well as distribution of expected background shower events from atmospheric neutrinos are shown in Fig. 6. About one event per year with shower energy more than 100 TeV from astrophysical neutrino flux is expected, comparing to 10 events in IceCube.

3. THE FIRST STAGE OF DEMONSTRATION CLUSTER

In April 2011 the first autonomous engineering array which includes pre-production modules of all elements, measuring and communication systems, as well as prototype of acoustic positioning system of GVD-cluster, was installed

and commissioned in Lake Baikal [15, 16]. The array was connected to shore by electro-optical cable which was deployed also in 2011. In April 2012 the next version of engineering array which comprises 36 OMs was deployed in Lake Baikal [17]. This array consists of two short strings and the first full-scale string of the GVD demonstration cluster with 24 OMs.

The next important step toward realization of the GVD project was made in 2013 by deployment of enlarged engineering array — the first stage of the demonstration cluster, which comprises 72 OMs arranged on three 345 m long strings, as well as instrumentation string with an array calibration and environment monitoring equipment [18]. The schematic view of this array is shown in Fig. 7. The vertical spacing of OMs is 15 m and the horizontal distance between strings is about 40 m. In addition to OMs, each string comprises the communication module (CoM) and two central modules of the sections. Also each string comprises one transmitter and three receivers of acoustic positioning system (AM) [19]. The modified cluster DAQ-center is located at the separate cable station and is connected to shore by the electro-optical cable. Instrumentation string is located at about 100 m from the measuring strings with OMs. It comprises the calibration laser source, eight optical modules, as well as 10 acoustic sensors of positioning

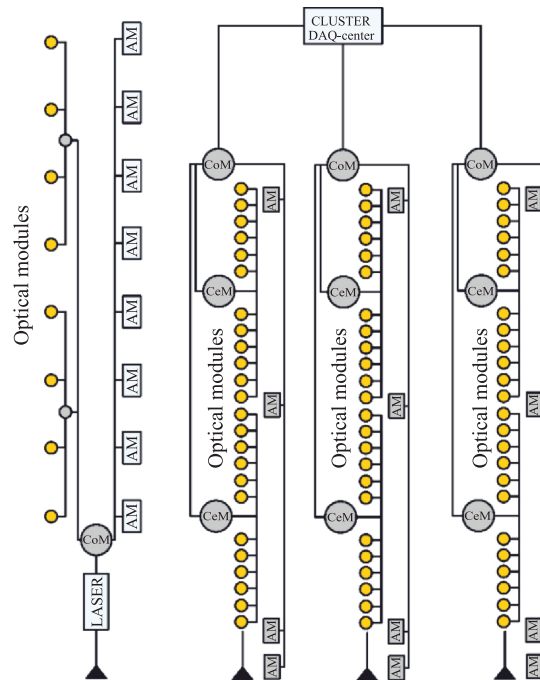


Fig. 7. Schematic drawing of the 2013 year engineering array

system. The calibration laser source [12] is located at 1215 m depth and is used for time synchronization between OMs on different strings. High intensity of laser source (up to $6 \cdot 10^{13}$ photons/pulse) allows illumination of OMs at distances of more than 200 m from the source. Acoustic sensors are arranged along the instrumentation string starting from the 50 m depth to the bottom of the string and perform monitoring of the string displacements at different depths caused by deep or/and surface water currents. Eight optical modules housing R8055 or XP1807 PMTs are arranged at depths from 600 to 900 m on the instrumentation string and aim at monitoring of the light background at these depths.

The first stage of demonstration cluster was successfully operated from April 2013 to February 2014 in several testing and data taking modes. A total of $5.5 \cdot 10^7$ events have been recorded which relate to 216 days of lifetime. Figure 8, *a* gives an indication of the data taking efficiency during 2013. Shown in Fig. 8, *b* is a time difference between two consecutive events of data sample. The exponential behavior of this distribution is consistent with expectation for randomly distributed experimental events and illustrates quality of data. Long-term control and monitoring of the array measuring system behavior, as well as background conditions during array operation in 2013, have been performed.

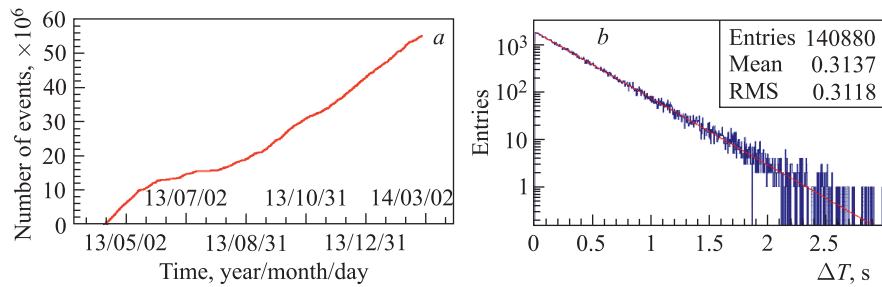


Fig. 8. *a*) Integrated number of recorded events since April 2013. *b*) Time difference between two consecutive events

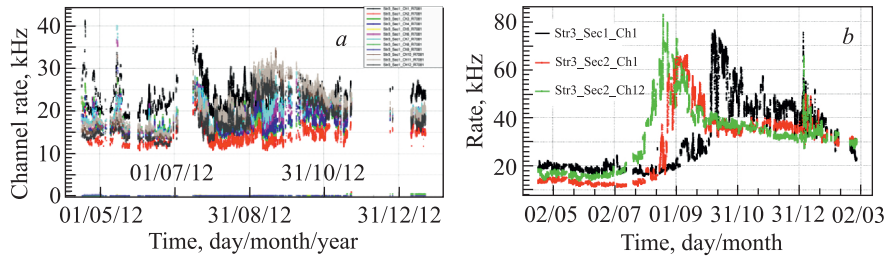


Fig. 9. *a*) Counting rates of OMs on the bottom section of the string which were observed in 2012. *b*) Counting rates of OMs 1, 13 and 24 on the string which were observed in 2013

In Fig. 9 the PMTs counting rates in 2012 (*a*) and 2013 (*b*) are shown. The main contribution to recorded counting rates is made by radiation produced by chemiluminescence in the deep water. During April–August 2013 the PMTs counting rates are about 10–20 kHz, which are comparable with values obtained in 2012. In August–November 2013 the rise of counting rates were indicated at different depths. The counting rates behavior in this period is consistent with the movement of approximately 200 m thick layer of water with high level of background light from top to bottom with a speed of 6–7 m/day.

One of the main goals of the array operation in testing modes was an estimation of the ability of in-situ calibration procedures. Calibration of the array recording system includes charge and timing calibrations of the measuring channels and time synchronization of OMs on different sections. All these calibration procedures are based on the usage of OM's internal calibration LEDs and the external laser light source.

The charge calibration enables one to translate the signal amplitudes into number of photoelectrons (p.e.), which is the relevant information for muon and shower energy reconstruction. For charge calibration of PMTs a standard procedure based on an analysis of a single photoelectron spectrum (s.p.e.) has been applied. In this calibration mode the pulses of two LEDs of OM are used. Intensity of the first LED is fitted to provide a detection of s.p.e. signals with detection probability about 10%. These pulses are used to measure s.p.e. distribution of channel signals. Pulses of the second LED with intensities corresponding to about 50 p.e. of PMT's signal are delayed for 500 ns and are used as a trigger to suppress background signals with small amplitudes initiated by PMT dark current, as well as light background of the lake deep water. Figure 10, *a* illustrates this procedure. In Fig. 10, *b* charge distribution of s.p.e. signals of one of the PMTs is shown.

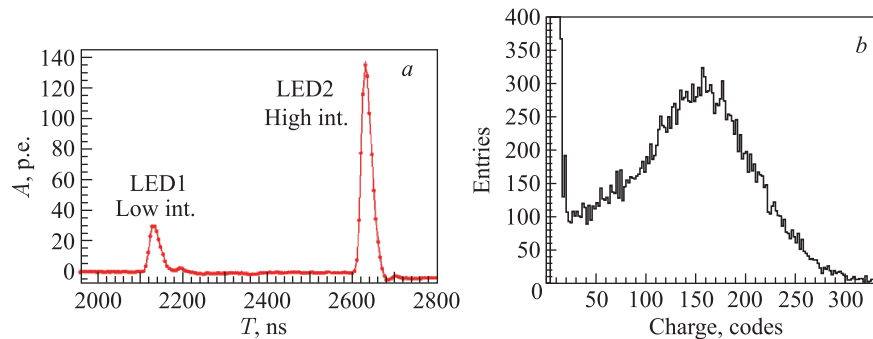


Fig. 10. *a*) Illustration of s.p.e. signal selection procedure. *b*) Charge distribution of s.p.e. signals of one of the PMTs

An optical activity from chemiluminescence of deep Lake Baikal water produces single photons at the photocathode level. Alternate procedure of charge calibration uses these noise events to study the single photoelectron peak.

The time calibration of measuring channels aims at control of the relative offsets in times between PMTs, which are formed by PMTs internal delay and delay caused by signal passing through about 90 m long cable connecting OM and CeM. Cable delays are measured once in the laboratory and are the same during array operation. PMT delay depends on a power voltage and thus it requires regular calibration during array operation. There is a reference pulse which is generated by OM controller and is delivered to the point of signal generation in PMT preamplifier. Reference pulse initiation is synchronized with the start time of LED. From measured difference between arrival times of LED signal and reference pulse the PMT delay is obtained. Figure 11, *a* illustrates this procedure.

Intensities of LEDs light bursts are high enough to illuminate the neighboring PMTs on the string. It allows a synchronization between OMs of different sections, as well as measurement of relative time offsets between channels inside one section. The time synchronization of different sections were performed and relative offsets between PMTs were derived by means of LEDs using known locations of strings and OMs obtained from analysis of data accumulated by the acoustic positioning system. Figure 11, *b* illustrates the time calibration of two neighboring PMTs by means of LED, located in one of them.

The performance and quality of using calibration procedures have been verified by a reconstruction of the position and intensity of the calibration laser source. An external calibration laser provides five series of 480 nm light pulses at five fixed intensity levels ranging from approximately 10^{12} to $6 \cdot 10^{13}$ photons/pulse [12], which corresponds to shower energies from 10 to 600 PeV. This

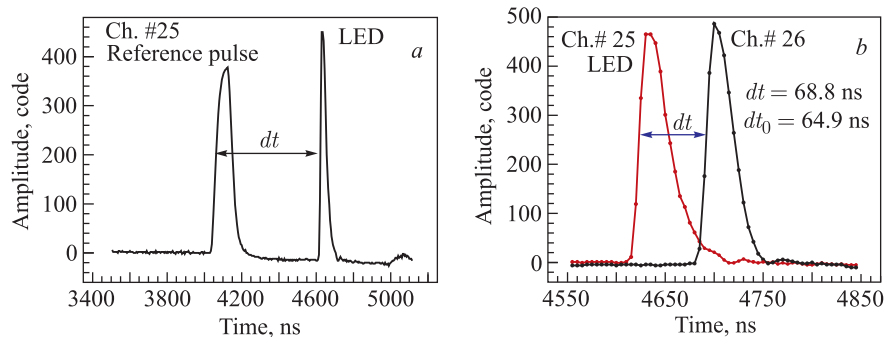


Fig. 11. *a*) Time distributions of the LED and reference signals which are used for measurement of the PMT intrinsic delay. *b*) Signals of PMTs #25 and #26 caused by LED located in OM #25. Expected time difference $dt_0 = 68.8$ ns and detected one $dt = 64.9$ ns, the relative offset is equal to 3.9 ns

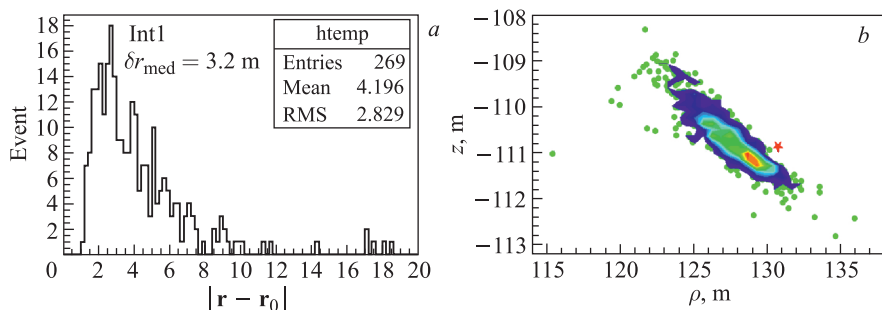


Fig. 12. *a*) Deviation of reconstructed laser coordinates from those obtained by the acoustic positioning system. *b*) Reconstructed laser positions on (ρ, z) -coordinates plane. Here z — vertical coordinate, ρ — horizontal distance from second string. Star indicates laser location obtained by the acoustic positioning system

allows one to test the array ability for high-energy cascades detection and reconstruction. Location of the laser source was reconstructed using arrival times of photons detected by PMTs, taking into account the timing calibration of PMTs. Results of reconstruction were compared with the laser coordinates obtained by the acoustic positioning system. Differences between the reconstructed coordinates and those obtained by the acoustic positioning system are shown in Fig. 12, *a*. Reconstruction accuracy (median value) is about 3 m. Shown in Fig. 12, *b* are reconstructed laser positions on (ρ, z) -coordinates plane. Here z is a vertical coordinate, ρ is a horizontal distance from the second string and the star indicates the laser location obtained by the acoustic positioning system.

Reconstruction of the laser intensities were performed by using calibrated amplitudes of hit PMTs and taking into account a reconstructed position of the laser source. Reconstructed intensities of four different series of the laser bursts are shown in Fig. 13, *a*. Relative uncertainty of intensity reconstruction is less

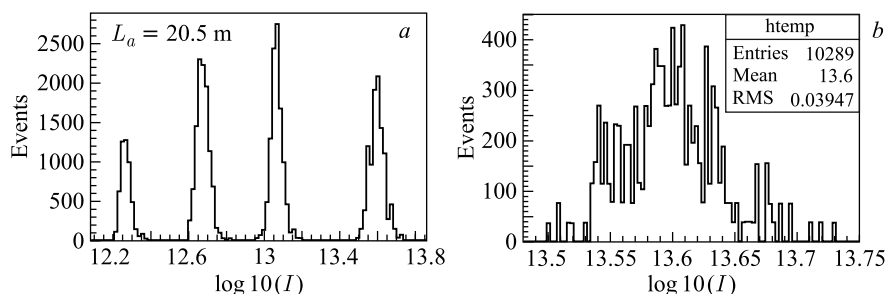


Fig. 13. *a*) Reconstructed intensities of four series. *b*) Reconstructed intensities for the most intensive series of the laser bursts

than 10% (see Fig. 13, *b*). The obtained results of reconstruction of the position and intensity of the laser source prove an expected quality of the array calibration procedures.

CONCLUSIONS

The construction of a km³-scale neutrino telescope — the Gigaton Volume Detector (GVD) in Lake Baikal — is the central goal of the Baikal Collaboration. During the R&D phase of the GVD project in 2008–2010 the basic elements of GVD — new optical modules, FADC readout units, underwater communications and trigger systems — have been developed, produced and tested in situ by long-term operating prototype strings in Lake Baikal. The prototyping phase of the GVD project has been started since April 2011 and aimed at construction and deployment in 2015 of the first demonstration cluster of GVD. The first stage of GVD-cluster which comprises three strings was deployed and successfully operated in 2013. In 2014 the second stage of demonstration cluster which consists of 112 OMs arranged at 5 strings has been deployed in Lake Baikal.

Acknowledgements. This work was supported by the Russian Foundation for Basic Research (grants 13-02-12221, 14-02-00972).

REFERENCES

1. *Avrorin A. et al. (Baikal Collab.)*. Asp-15: A Stationary Device for the Measurement of the Optical Water Properties at the NT200 Neutrino Telescope Site // *Nucl. Instr. Meth. A*. 2012. V. 693. P. 186.
2. *Aynutdinov V. et al. (Baikal Collab.)*. Search for a Diffuse Flux of High-Energy Extraterrestrial Neutrinos with the NT200 Neutrino Telescope // *Astropart. Phys.* 2006. V. 25. P. 140.
3. *Avrorin A. et al. (Baikal Collab.)*. Search for High-Energy Neutrinos in the Baikal Neutrino Experiment // *Astron. Lett.* 2009. V. 3.5. P. 651.
4. *Belolaptikov I. A. et al. (Baikal Collab.)*. The Baikal Underwater Neutrino Telescope: Design, Performance and First Results // *Astropart. Phys.* 1997. V. 7. P. 263.
5. *Aynutdinov V. M. et al. (Baikal Collab.)*. Search for Relativistic Magnetic Monopoles with the Baikal Neutrino Telescope // *Astropart. Phys.* 2008. V. 29. P. 366.
6. *Avrorin A. V. et al. (Baikal Collab.)*. An Experimental String of the NT1000 Baikal Neutrino Telescope NT200 // *Astron. Lett.* 2011. V. 3.7. P. 692.
7. *Aynutdinov V. et al. (Baikal Collab.)*. The BAIKAL Neutrino Experiment: Physics Results and Perspectives // *Nucl. Instr. Meth. A*. 2009. V. 602. P. 227.
8. *Avrorin A. et al. (Baikal Collab.)*. The Baikal Neutrino Experiment // *Nucl. Instr. Meth. A*. 2011. V. 626. P. S13.

9. *Avrorin A. et al. (Baikal Collab.)*. The Baikal Neutrino Telescope: Results and Plans // Nucl. Instr. Meth. A. 2011. V. 630. P. 115.
10. *Avrorin A. et al. (Baikal Collab.)*. The Gigaton Volume Detector in Lake Baikal // Ibid. V. 639. P. 30.
11. *Avrorin A.V. et al. (Baikal Collab.)*. An Experimental String of the NT1000 Baikal Neutrino Telescope // Instr. Exp. Tech. 2011. V. 54. P. 649.
12. *Aynutdinov A.V. et al. (Baikal Collab.)*. Baikal Neutrino Telescope // Phys. At. Nucl. 2006. V. 69. P. 1914.
13. *Aartsen M. G. et al. (IceCube Collab.)*. Evidence for High-Energy Extraterrestrial Neutrinos at the IceCube Detector // Science. 2013. V. 342. P. 1242856.
14. *Aartsen M. G. et al. (IceCube Collab.)*. First Observation of PeV-Energy Neutrinos with IceCube // Phys. Rev. Lett. 2013. V. 111. P. 021103.
15. *Avrorin A. et al. (Baikal Collab.)*. Status of the Baikal-GVD Project // Nucl. Instr. Meth. A. 2012. V. 692. P. 46.
16. *Avrorin A. et al. (Baikal Collab.)*. Current Status of the BAIKAL-GVD Project // Nucl. Instr. Meth. A. 2013. V. 725. P. 23.
17. *Avrorin A. et al. (Baikal Collab.)*. Present Status of the BAIKAL-GVD Project Development // J. Phys. Conf. Ser. 2013. V. 409. P. 012141.
18. *Avrorin A. D. et al. (Baikal Collab.)*. The Prototyping/Early Construction Phase of the BAIKAL-GVD Project // Nucl. Instr. Meth. A. 2014. V. 742. P. 82.
19. *Avrorin A. V. et al. (Baikal Collab.)*. A Hydroacoustic Positioning System for the Experimental Cluster of the Cubic-Kilometer-Scale Neutrino Telescope at Lake Baikal // Instr. Exp. Tech. 2013. V. 56. P. 449.